Title
Composition of High-Energy Heavy-Ion Beams: Preliminary Measurements

Author
Maccabee, H D

Publication Date
2023-09-06

Composition of High-Energy Heavy-Ion Beams: Preliminary Measurements

H. D. Maccabee

Donner Laboratory and Lawrence Berkeley Laboratory
University of California
Berkeley, California 94720

No. of copies submitted: 3

Manuscript pages: 24

Figures: 9

Tables: None

DISCLAIMER

Running head:

High-Energy Heavy Ions

Proofs to be sent to:

Dr. H. D. Maccabee
Building 29, Room 213A
Lawrence Berkeley Laboratory
University of California
Berkeley, California 94720

Radiat. Res. ?, pp. ____-____, _____.

Composition of High-Energy Heavy-Ion Beams: Preliminary Measurements

H. D. Maccabee

Donner Laboratory and Lawrence Berkeley Laboratory
University of California
Berkeley, California 94720

November 1972

ABSTRACT

Silicon semiconductor detector systems were used to measure the energy deposition spectra of 240-MeV/nucleon oxygen ion beams at the Bevatron of Lawrence Berkeley Laboratory. The results are useful for determining the composition of the beam, before and after passing through varying thicknesses of water absorber. In particular, contamination of the incident oxygen beam by carbon ions on the order of 1% was detected and resolved. Secondary particles due to nuclear fragmentation in water were identified and quantified. The experimental estimate of the mean free path of fast oxygen ions in water is 20 g/cm^2, in agreement with calculations from cosmic ray data and geometric cross sections.

Key words:

Heavy ions

Fragmentation

Energy deposition

Beam composition

Nuclear secondaries

I. INTRODUCTION

Recently, high-energy, heavy-ion beams were produced for the first time at the Princeton Particle Accelerator and the Bevatron of the Lawrence Berkeley Laboratory(1). Because of their excellent depth-dose characteristics, and high LET-values after penetrating to depth in tissue, these beams could be very useful in tumor therapy and other applications of deep lesion production in biology and medicine(2). For such purposes, it is necessary to accurately identify the composition of the particle beam, in addition to conventional dosimetry by measuring ionization. In particular, our goal is to measure the amount and type of "contamination" of the incident beam (arising at the ion source or from collisions in the acceleration or beam transport systems), and to identify and quantify the secondary particles arising from nuclear interactions as the primary beam penetrates to depth in tissue-like absorbers. This information can be used to estimate the dose contribution due to contamination and secondaries. These points are significant because there has been some skepticism in the past about the usefulness of high-energy heavy-ion beams, by workers who envisioned an excessive amount of conversion of primary beam into non-useful secondary fragments.

II. METHOD

We have used the nitrogen and oxygen ion beams developed in channel 2 of the Berkeley Bevatron, schematically shown in Fig. 1. Although the maximum acceleration potential of the machine for these ions is 2 GeV per nucleon, we have used lower energy beams (240 to 280 MeV per nucleon), because these beams have a range suitable for Bragg-peak irradiation at a depth equivalent to half the thickness of

the human body. For example, the range of an oxygen-16 ion with kinetic energy 250 MeV/nucleon is 9.35 cm of water (see appendix). The lower-energy beams are obtained by extracting the internal beam before the full acceleration cycle is over. Grunder et al. have given more complete information on the acceleration of heavy ions at the Bevatron (1).

The basic method of studying beam composition is by observation of the energy-deposition characteristics of the beam component particles in semiconductor detectors, and combining this information with known acceleration characteristics and cosmic ray and particle physics data. In particular, the stopping power of a charged particle with a given velocity is proportional to the square of the particle charge number. The bending magnets of the beam transport system serve as velocity selectors for particles with a fixed charge-to-mass ratio. The charge-to-mass ratio is 1:2 for many of the ions of interest here (e. g., $^{4}_{2}He$, $^{10}_{5}B$, $^{12}_{6}C$, $^{14}_{7}N$, $^{16}_{8}O$, etc.), and particles are fully ionized at the incident velocities considered. Thus, for example, if ^{12}C, ^{14}N, and ^{16}O are present in the ion source, they will be accelerated and transported at the same velocity. Therefore their specific ionization values will be in the ratio of their z^2-values, and an energy-deposition measurement in a thin detector will serve to distinguish between them.

The problem of identifying secondary particles after nuclear interactions in an absorber is more difficult, because the velocity of the secondary is not fixed, and an energy-deposition measurement yields a value approximately proportional to (z^2/β^2). Furthermore, different isotopes with the same charge can result from the collisions, and the thin-absorber assumption may be violated (i. e., the particles may be slowed down such that the increase in stopping power within the detector

is not negligible). Although it is possible to construct elaborate particle-identifier "telescope" systems to cope with these problems (3), we have used a relatively simple approach in these preliminary studies, studies based on the inference from previous heavy-ion studies, e.g., at the Bevatron, that virtually all of the fragmentation collisions of high-energy heavy-ions result in secondaries that differ very little in velocity from the primary (4). This has been called the "$\Delta\vec{v} = 0$" approximation, which enables us to obtain useful identification of the charge numbers of secondaries, with the relatively simple detection system shown in Fig. 2.

Energy deposited by a charged particle is converted to a charge pulse in the "analyzing" semiconductor detector [3-mm Li-drifted silicon, in the "top-hat" configuration (5)]. Although there is some evidence that there is a small pulse-height defect for slow heavy ions in semiconductor detectors, and perhaps a slight shift in the value of the average energy per hole-electron pair, these corrections are assumed to be negligible for the fast heavy ions studied here. Thus, the charge collected is assumed to be directly proportional to the energy deposited. The pulse is converted by a charge-sensitive preamplifier to a voltage pulse, and transmitted via a long cable from the irradiation cave (channel 2) to the biomedical counting room where it is amplified and shaped. It is then fed into a coincidence and linear gate system which only accepts it for analysis if it is accompanied by another pulse from the "pile-up" rejector system. Pulse pile-up can be a severe problem under Bevatron operating conditions, where 40×10^3 heavy ions can be incident in a millisecond of beam-spill time, leading to instantaneous rates of 40 MHz. The pile-up

rejector inspects the first 2.5 microseconds after a fast-rising pulse for a second fast pulse rise, and rejects such a pile-up by not sending an output pulse to the gate. The "thin" detector coincidence requirement also serves to eliminate pulses due to particles passing through the edges of the sensitive region of the analyzing detector (where charge collection is not uniform) because its sensitive area is smaller. The sensitive diameter of the thin detector is 8 mm, compared to 12 mm for the analyzing detector, which is centered 1 cm downstream of the thin. Pulses from particles which are properly aligned and not pile-ups are thus fed into a 400-channel pulse-height analyzer.

Energy calibration of the system is achieved with a standard-amplitude pulse generator and known radioactive particle sources, by the usual methods of nuclear spectroscopy. There is some uncertainty here because of the problem of extrapolation from 8-MeV (natural alpha-particle sources) to measured energy depositions greater than 200 MeV. Thus, we also use information from the energy deposition of the known primary heavy-ion beam, as an internal calibration check.

Energy resolution capability for the system is better than 30-keV (FWHM), a negligible factor considering that the energy pulses analyzed are all greater than 3 MeV. The energy resolution has no significant effect on charge resolution. Dynamic range, however, can be a problem, given the desire to analyze pulses from 16_0 ions with energies such that they have a range of 3 mm in Si (about 800 MeV) as well as pulses from fast protons depositing only about 4 MeV (a factor of 200). Even for the incident beam, with all particles having about the same velocity, a dynamic range of 64 is necessary to account for the difference in z^2 between protons and

oxygen ions. Thus one must vary amplifier gain extensively for different experimental runs.

III. RESULTS

The experimental data, in the form of counts per channel versus channel number, are processed with calibration information to yield a plot of the energy-deposition frequency spectrum. Since statistical error in the absolute value of the peak height is of little interest here, error bars have not been plotted, and smooth curves have been drawn through the data points for convenience in distinguishing peaks. The following spectra are results selected from a number of experiments performed on 29 January and 1 February, 1972.

Figure 3 shows the energy deposition frequency spectrum of the "incident" oxygen ion beam (240 MeV/nucleon) measured in the 3 mm of silicon (0.7 g/cm^2) of the analyzing detector, obtained after passage through the beam pipe exit window, 110 cm of air path, and the "thin" detector (0.033 g/cm^2 Si). There is a pronounced peak at a (most probable) energy deposition of 149 MeV, indicating that oxygen ions entering the detector at 3.84 GeV total kinetic energy would be exiting at 3.69 GeV (or about 230.7 MeV/nucleon). This energy deposition corresponds well to the calculated value of energy loss of 240 MeV/nucleon oxygen ions in 0.7 g/cm^2 Si, 147 MeV, obtained from range tables generated by Bichsel's code (see appendix). The peak has a full width at half-maximum of 6.7 MeV, and a "tail" corresponding to smaller energy deposition. There is also a distinct "bump" centered at energy deposition 84 MeV. This can be identified as due to carbon ions at the same velocity as the oxygen ions, since, at the same velocity, the pulse heights will be in the ratio of the z^2 values which is.

36:64 = 0.562, and (0.562) (149 MeV) = 83.8 MeV. This small peak is associated with the contamination of the nominal oxygen beam by carbon, arising from the fact that CO_2 gas had been present in the ion source. The number of counts under the carbon peak, when compared to the number under the oxygen peak, indicates that the contamination amounted to about 1.3% (by number of particles) in this instance.

Figure 4 shows the energy-deposition frequency spectrum in the same analyzing detector after passing the beam through the exit window, air path, three ionization chambers, monitor and quadrant scintillators, the two end windows of the (empty) variable water column, and the "thin" detector, such that the residual beam energy is about 216 MeV/nucleon. The main peak is at a most probable energy deposition of 161 MeV, indicating that oxygen ions entering the detector at 3.46 GeV would be exiting at 3.30 GeV (or 206 MeV/nucleon). This energy deposition is consistent with the calculated value, approximately 160 MeV. Now the events under the carbon peak are about 2.5% of those under the oxygen peak, possibly indicating an increase due to carbon ion secondaries generated in the absorber materials. There is also a "bump" which probably corresponds to helium ion secondaries generated by nuclear collisions in the materials upstream.

The experimental conditions for the data in Fig. 5 are similar to those above with the substitution of two scintillation counters for one of the ionization chambers upstream, but in this case the variable water column has 2 cm of H_2O (i.e., 2 g/cm^2), and the residual beam energy of the oxygen ions incident on the analyzing detector is about 178 MeV/nucleon. Amplifier gain (i.e., channel number/energy deposited) has been reduced by a factor of 2.0. The measured value of the energy deposition (most probable) in the

oxygen ion peak is 180 MeV, compared to a calculated value of 178 MeV. The peak width is 9.7 MeV (FWHM), and there are: peaks corresponding to nitrogen ion secondaries depositing around 139 MeV; carbon ions as before; some structure probably due to Li, Be, and B ions; a helium peak; and a possible proton peak, which is unresolvable due to noise in the first channel.

Finally, three more cm of H_2O are added to the water column (for a total of 5 g/cm^2), and the resulting energy-deposition frequency spectrum is shown in Fig. 6. The main peak from the oxygen ions (calculated incident energy, 110 MeV/nucleon; calculated energy deposition, 260 MeV) is off scale here, and we concentrate on the bumps due to the lighter secondaries. The nitrogen peak is now well defined, with a most probable energy deposition of about 168 MeV, compared to a calculated value of about 175 MeV, obtained with the simplifying assumption that the most probable nitrogen secondary is generated with an energy of 180 MeV/nucleon at a depth of 2 cm in the water column and slows down in 3 cm of H_2O before impinging on the detector.

The carbon peak is bimodal, with a sharp edge at most probable energy deposition 105 MeV, which is associated with the fastest (smallest energy deposition) carbon ions, i. e., the contamination from the source, which is generated at the same velocity as the primary oxygen ions. Calculations of the position of the peak based on this assumption yield a value of about 107 MeV. The maximum in the broader portion of the peak occurs at 118 MeV, which is consistent with a calculated value of 120 MeV, obtained from the approximation that the most probable secondary is generated with an energy of 180 MeV/nucleon at a depth of 2 cm in the water

column and slows down in 3 cm of H_2O before entering the analyzing detector.

The peak which is tentatively identified with lithium, beryllium, and boron secondaries is not resolved into components but has a maximum around .77 MeV. There is also a narrow peak which is tentatively identified as helium secondaries but is incompletely resolved from a large spike (off scale at 1076 counts in maximum channel) which is identified as protons.

Discussion

There are several physical phenomena which affect the shapes of the peaks in the energy-deposition spectra. The most obvious is that of energy straggling. For the primary ion beam, which is extracted and transported with a small momentum spread (< 1%), there are fluctuations of energy loss in various absorbers upstream of the analyzing detector, leading to variation in the energies of the incident particles. For a given incident energy, there is also straggling of energy deposition in the detector itself. This effect should be greater than the two previously mentioned. For example, for a 240-MeV/nucleon oxygen ion passing through 0.7 g/cm^2 Si, one expects the Vavilov parameter kappa to be:

$$\kappa = 0.150\ z^2 s\ (Z/A)\ [(1-\beta^2)/\beta^4] = 15.9$$

where s = absorber thickness in g/cm^2; see ref. (6) for a discussion of straggling in thin absorbers.

$\kappa = (0.15)(1^2)(0.7)(0.5)[0.634/0.1335] = 15.9$.

Since the fraction of kinetic energy loss $\Delta T/T = (149)/(16)(240) = 0.039$, the Bohr solution for thin absorbers is valid, with a Gaussian energy-loss distribution characterized by variance

$$\sigma^2_{Bohr} = 0.157\ z^2 s\ (Z/A) \text{ in } (MeV)^2 = 3.52\ (MeV)^2,$$

$$\therefore \text{FWHM} = 2.36\ \sigma = (2.36)\ (1.88) = 4.2 \text{ MeV}.$$

This width accounts for less than half (by quadrature) of the total width of the measured peak in Fig. 3, however, and one is forced to look elsewhere for an explanation of the discrepancy.

Energy straggling is also reflected in the energy deposition of the secondaries, in terms of the fluctuations of energy loss of the primary before the collision which generates a secondary, the fluctuations of energy loss of the secondary before entering the detector, and the energy loss straggling in the detector itself. Much more important than these effects, however, is the variation in depth in absorber at which the nuclear interaction (which generates a secondary) takes place. Since the secondary fragment generally has a smaller charge number than the primary, if it is emitted with the same velocity (the "$\Delta \vec{v} = 0$" approximation) it will have a smaller specific energy loss (proportional to z^2). This is a greater factor than the decrease in total kinetic energy (roughly proportional to z), and its residual range (proportional to A/z^2) will be greater than that of the primary. The net result is that at any point in an absorber, there will be a distribution of velocities of secondaries of a given type, with the slowest corresponding to those which have been generated nearby from primary collisions and the fastest corresponding to those which were generated at the entry point of the absorber and have been losing speed more slowly than the primary.

the longest path.

Thus, the larger values in the energy-deposition spectrum for a particular fragment type correspond to the slowest secondaries (generated nearby), and the smaller energy-deposition values correspond to the fastest (generated at entry), with the extreme example being contamination of the primary beam entering the absorber at the same velocity as the primaries (e. g., the carbon contamination spike in Fig. 6). These peak-broadening effects increase with depth of absorber, and are also broadened themselves by the increased energy straggling with depth, and by the effect that some of the secondaries are probably generated with speeds significantly less than the primaries, i. e. $\Delta \vec{v} \neq 0$.

There is another effect which tends to alter the energy-deposition spectrum, related to the fact that there is a certain probability that a fast heavy ion will undergo a nuclear interaction in the detector itself, generating lighter fragments which, if emitted at the incident velocity, will have a <u>total</u> energy deposition in the remaining detector thickness which is less than that of the incident ion. This is evident from a generalization of the example of an ion of charge z breaking into fragments of charge z_1 and z_2, such that $z = z_1 + z_2$. Since $z^2 = z_1^2 + z_2^2 + 2z_1z_2$, z^2 is always greater than the sum of z_1^2 and z_2^2. The net result of this effect is the formation of energy-deposition events which are smaller than the events from passage of the incident ions through the detector without fragmentation; a lower-energy-deposition "tail" is formed on the peak from any type of ion, and the peak is itself broadened. Note that the formation of a low-energy-deposition tail from this effect is the opposite of the high-energy-loss tail formed in

the Landau effect and in thick-absorber energy straggling. This nuclear effect is believed to account for the smaller-energy-deposition tail seen in Figs. 3 and 4, for the oxygen ion peak, and for a significant broadening of the peaks. One must also remember that the above argument is slightly vulnerable to the exceptions due to fragment formation with significant speed loss, and nuclear "star" event formation in the detector, which would tend to cause larger energy deposition.

We can estimate the importance of the nuclear interactions in the detector by calculating the probability of an interaction per passage of oxygen ion through 3 mm ($0.7 g/cm^2$) of silicon, from the mean free path of O on Si, using the Bradt and Peters expression (7):

$$\lambda\ (1 \text{ on } 2) = 25 A_2 / (A_1^{1/3} + A_2^{1/3} - 1.17)^2\ g/cm^2,$$

$$\lambda\ (\text{O on Si}) = 36.3\ g/cm^2.$$

Thus the interaction probability is

$$1 - e^{-x/\lambda} = 1 - e^{-0.7/36.3} = 0.019.$$

This estimate (2% interacting in the detector) is probably too small.

Errors

The results shown must be qualified by our knowledge of several sources of significant errors. The nature of the electronics (e.g., dynamic range limitations, discriminator threshold settings against noise, etc.) is such that there are losses of pulses due to the sparsely ionizing particles, i.e., protons, deuterons, and He ions. Furthermore, if a singly-charged secondary comes through the system simultaneous

with a heavier fragment, its contribution to the pulse height will be "buried" with the larger contribution of the multiply-charged ion, resulting only in a slight shift to the right of the peak from the heavier fragment. This bias against the low-z secondaries is compounded by the size and geometric arrangement of the detectors, which register only particles in the "straight-ahead" direction from the water absorber (target). If there is significant lateral scattering after a fragmentation collision, the lightest fragments are likely to be scattered most, and therefore would tend to miss the detectors (20 cm downstream). We expect that these effects will result in a severe underestimation of the number of fragments with z = 1, and a moderate underestimation of the fragments with z = 2. It might be possible to estimate the error in the amount of low-z secondaries by simple considerations of charge conservation in a collision, e.g., fragmentation of an oxygen ion into a nitrogen should be accompanied by a singly-charged fragment.

There are other errors involved, such as the energy calibration error resulting from extrapolation from low-energy natural alpha particle sources, etc., but this type of error does not result in misidentification of a peak or loss of counts in a peak. There is also error possible in the number of counts in the lowest channels, due to noise from the detector and electronics, but we are not placing much importance on the smallest pulses here, due to our previous arguments on losses of low-z secondaries. Another "error" results from the fact that we have not designed our experiment to detect neutral secondaries or contamination (especially neutrons) and have made no attempt to identify mesons. For example, a charged pion emitted in the straight-ahead direction could be mistaken for a proton, or even a heavier secondary, if it interacts in the analyzing detector to form a "star."

IV. COMPARISON WITH THEORY AND OTHER MEASUREMENTS

In general, these preliminary measurements tend to confirm our expectations that the nuclear fragmentation process would not "spoil" the high-energy heavy-ion beam for biomedical purposes. The results are consistent, for example, with the predictions of S. B. Curtis, that the secondary-particle contribution to the Bragg peak of a 300-MeV/nucleon neon beam would be less than 15% in width or height.[1]

We can make some particular comparisons with the results of other heavy-ion experiments and cosmic ray data interpretation. In August 1971 and January 1972, nitrogen ion beams were developed at the Bevatron, and fragmentation of 2.1-GeV/nucleon ^{14}N nuclei in carbon and hydrogen was studied and reported by Heckman et al. (4, 8). They concluded that the preliminary values of the partial differential cross sections at 0° give evidence that the modes of fragmentation of ^{14}N projectiles are independent of the target nucleus. Also the Heckman group used their nine-detector telescope to study the fragmentation of a 280-MeV/nucleon ^{14}N beam impinging on a 5-cm water absorber after passing through the usual vacuum windows, monitor scintillator, etc., resulting in degradation to a residual energy of 160 MeV/nucleon for N ions entering the first silicon detector. This is approximately equivalent to analyzing the residual beam at a depth of 5 cm of soft tissue in a patient being irradiation with 240-MeV/nucleon N ions. Their raw data in the form of 711 particle "signatures," were analyzed by this author, with the results shown in an event-

frequency histogram in Fig. 7. The most apparent result is that the great majority (80%) of the impinging N ions emerge from the absorber as slower N ions (i.e., without nuclear fragmentation). Seventy percent stop in the telescope at the end of their range, and 10% undergo nuclear reactions in the silicon. The 20% which undergo fragmentation in the absorber result in secondaries emerging such that 2% of the events are associated with singly charged particles (this is probably underestimated severely), 4% He, 1% each of Li, Be, and B, and 4% C. Fragmentation into carbon is favored, according to the alpha-particle model of the nucleus, which treats a nitrogen nucleus as three alphas (^{12}C) plus a deuteron. The interpretation of the events labeled with a question mark is open to doubt. They had signatures indicating higher ionization than the primary N beam, and could have resulted from a 7% oxygen contamination of the incoming beam, or superposition (coincidence) of a primary with a lighter fragment, etc.

From these data we can obtain estimates of cross sections, mean free path, and fragmentation parameters for comparison with the predictions from cosmic ray data. From our analysis of the data of Heckman et al. on 280 MeV/nucleon nitrogen in water, 5 with 565 out of 711 ^{14}N ions surviving after 5-g/cm^2 H_2O, we extract a mean free path for fragmentation of $\lambda(N \text{ on } H_2O) \approx 22(\pm 30\%)$ g/cm^2.

$\lambda(N \text{ on } H_2O) \approx 22(\pm 30\%)$ g/cm^2.

This compares very well with the predicted value of 21 g/cm^2 calculated from Waddington's[9] $\lambda(N \text{ on } H) \approx 6.7$ g/cm^2 and $\lambda(N \text{ on } O) \approx 28.4$ g/cm^2 obtained from Bradt and Peters.[7] Similarly, from 497 of 565 ^{14}N ions surviving after stopping in about 5.5-g/cm^2 silicon, we extract a mean

free path of

$$\lambda(\text{N on Si}) \approx 43(\pm 30\%)\ \text{g/cm}^2 .$$

This compares reasonably with 38 g/cm^2, the prediction from the geometric cross section. Some disagreement is expected from the fact that the geometric cross section is only valid at high energies, e.g., $\gtrsim$ 1-GeV/nucleon, while the data are taken from interactions with projectile energies from 160 MeV/nucleon to zero.

Estimates of the mean free path of oxygen ions in water can be obtained from our data, by comparing the number of events under the fragment peaks with the number remaining in the primary peak. For example, in a run with 4-cm water absorber, 2500 fragmentations were observed while 11,400 primaries were transmitted; i.e., a total of 13,900 primaries were incident, leading to a mean free path estimate of

$$\lambda(\text{O on } H_2O) \approx 20\ \text{g/cm}^2 \pm 30\% .$$

This is consistent with the experimental value for nitrogen ions, since the oxygen nucleus has about 10% larger area, and agrees well with the value 19.3 g/cm^2 calculated from Waddington's λ(O on H) $\approx$ 6 g/cm^2 and λ(O on O) $\approx$ 26.7 g/cm^2 from Bradt and Peters.

Furthermore, by rough calculation from the data shown in Fig. 6, we can estimate that the fragmentation probabilities are about the same (± 50%) for the five groups of fragments: N, C, L-nuclei (i.e., B, Be, and Li lumped together), He, and H. This does not agree with expectations (see, for example, Fig. 1 of Curtis), but is consistent with the values used by Lyman (unpublished data, 1972) for best fit to the number-distance and ionization vs. depth data for the oxygen ion beam in water.

V. CONCLUSIONS

We have drawn the following provisional conclusions from the preliminary experiments and data described above.

1. Semiconductor detector systems are an adequate method of measuring the amount and type of "contamination" of incident high-energy heavy-ion beams, and can be used to identify and quantify the secondary particles arising from nuclear fragmentation as the primary beam penetrates to depth in tissue-like absorbers.

2. The number of nuclear secondaries created in thicknesses up to 5 cm of tissue-equivalent material is small with respect to the number of primaries remaining in the beam; the contribution to the depth-dose curve will be even smaller, given the decreased nuclear charge of the fragments.

3. The measured mean free paths for nuclear fragmentation of high-energy heavy-ion beams in water agree (within experimental errors) with the values calculated from geometric cross sections and cosmic ray data, but fragmentation parameters may disagree with previous expectations.

4. In terms of radiation physics, the Bevatron high-energy heavy-ion beams appear to have desirable characteristics for continuing research on biomedical applications.

ACKNOWLEDGMENTS

This work is dedicated to the memory of Professor Aharon Katchalsky (Katzir), who was assassinated by terrorists at the Tel Aviv Airport on May 30, 1972. He was a brilliant scholar and teacher, a wonderful friend and colleague, and an inspiration to all of us associated with the biophysics program at Berkeley.

I would like to thank the following people for their contributions to this work: Fred Goulding, Don Landis, Jack Walton, and Stu Wright for help with detectors and electronics; Stan Curtis, Walter Schimmerling, Mike Goitein, and Hans Bichsel for useful discussions and calculations; Harry Heckman, Doug Greiner, Pete Lindstrom, and Fred Bieser for furnishing their data on nitrogen fragmentation; and C. A. Tobias for his continued support and encouragement. I also want to express my gratitude to Ed Lofgren, Herman Gründer, Walt Hartsough and the crew of the Bevatron, for their cooperation in producing high-energy heavy-ion beams, which make this work possible.

This work was supported by the U. S. Atomic Energy Commission.

APPENDIX: RANGE AND STOPPING POWER OF HIGH-ENERGY HEAVY IONS IN WATER

In view of the fact that accelerated high-energy heavy-ions became available only recently, there was little need for precise calculations of their energy-loss characteristics. Now, however, there is a need for such data. The computer code RANGE[2] calculates the range and stopping power of fully stripped ions of arbitrary isotopes of elements from hydrogen through neon, and furnishes results in the form of computer printout tables for specific energies from 0.05 to 1000 MeV/nucleon, in arbitrary stopping materials. For the use of other investigators, we have plotted these data logarithmically, for water absorbers, based on an effective atomic number Z = 7.0, atomic weight A = 12.6, and mean excitation potential I = 64.85 eV. Figure 8 shows the range of ions in water as a function of specific energy (MeV/nucleon) for ^{1}H, ^{4}He, ^{9}Be, ^{12}C, ^{16}O, ^{20}Ne, ^{40}Ar, and ^{56}Fe. The values for Ar and Fe were obtained by A/z^2 scaling from lighter ions at the same velocity, i.e., the same specific energy. Note that the range of fast ^{4}He ions is the same as for protons at the same velocity. Figure 9 shows the stopping power (LET_{∞}) of ions in water as a function of specific energy (MeV/nucleon) for He, Li, Be, B, C, N, O, Ne, Ar, and Fe. Values for Ar and Fe were obtained by z^2 scaling from lighter ions at the same velocity. Note that energy loss of oxygen beams in silicon detectors can be calculated from the fact that the mass stopping power of fast oxygen ions in Si (in MeV/g/cm^2) is nearly identical to that of nitrogen ions in H_2O.

REFERENCES

1. M. G. White, M. Isaila, K. Prelec and H. L. Allen, Heavy Ion Acceleration, Science 174, 1121-1123 (1971). H. A. Grunder, W. D. Hartsough, and E. J. Lofgren, Acceleration of heavy ion beams at the Bevatron. Science 174,1128-1129 (1971).

2. C. A. Tobias and P. W. Todd. Heavy Charged Particles in Cancer Therapy, in Radiobiology and Radiotherapy, National Cancer Institute Monograph No. 24 (1967).

3. D. E. Greiner, A versatile high-resolution particle identifier theory. Nucl. Instr. Methods 103 291-308 (1972).

4. H. H. Heckman, D. E. Greiner, P. J. Lindstrom, and F. S. Bieser, Fragmentation of nitrogen-14 nuclei at 2.1 GeV per nucleon. Science 174, 1130 (1971).

5. F. S. Goulding, Semiconductor detectors for nuclear spectrometry. Nucl. Instr. Methods 43, 1-54 (1966).

6. H. D. Maccabee, M. R. Raju, and C. A. Tobias, Fluctuations of energy loss by heavy charged particles in thin absorbers, Phys. Rev. 165 469-474 (1968).

7. H. L. Bradt and B. Peters, The heavy nuclei of the primary cosmic radiation. Phys. Rev. 77, 54-70 (1950).

8. H. H. Heckman, D. E. Greiner, P. J. Lindstrom, and F. S. Bieser, Fragmentation of N-14 nuclei at 29 GeV. Phys. Rev. Letters 28, 926-929 (1972).

9. C. J. Waddington, Composition of the primary cosmic radiation. In Progress in Nuclear Physics, (O. R. Frisch, ed.), Vol. 8, p. 32, Pergamon, New York, 1960.

FOOTNOTES

[1] S. B. Curtis, "Secondary Contributions to the Bragg Peak of a High-Energy Heavy-Ion Beam", p. 171 in Donner Laboratory Semiannual Report UCRL-18347. University of California, Lawrence Radiation Laboratory (1968).

[2] H. Bichsel, "A Fortran Program for the Calculation of Energy Loss of Heavy Charged Particles", Lawrence Radiation Laboratory Report UCRL-17538 (1967). Method described in: H. Bichsel, "Passage of Charged Particles Through Matter", Amer. Inst. of Physics Handbook, Third Ed., McGraw-Hill, New York (1972).

Figure Legends

Fig. 1. Schematic plan view of the Bevatron.

Fig. 2. Schematic diagram of Silicon Detector System.

Fig. 3. Energy-deposition spectrum of "virgin" beam of 240-MeV/nucleon oxygen ions in 3 mm (0.7 g/cm^2) Si.

Fig. 4. Energy-deposition spectrum of oxygen ion beam after passing through three ionization chambers, monitor and quadrant scintillators, and empty water column; residual energy about 216 MeV/nucleon.

Fig. 5. Energy-deposition spectrum of oxygen ion beam after passing through two ionization chambers, three scintillators, and water column containing 2 cm H_2O.

Fig. 6. Energy-deposition spectrum of secondaries generated by passing oxygen ion beam through ionization chambers, monitor scintillator, and water column containing 5 cm H_2O.

Fig. 7. Event-frequency histogram of 280 MeV/nucleon ^{14}N ions fragmenting in 5 cm H_2O, etc. From our analysis of data taken by Heckman et al. (unpublished).

Fig. 8. Range of ions in water as a function of specific kinetic energy, in MeV/nucleon. Values from Bichsel's code ation of Bichsel's RANGEANGE.

Fig. 9. Mass stopping power (LET_∞) of heavy ions in water as a function of specific kinetic energy, in MeV/nucleon. Values from Bichsel's code RANGE. Bichsel's code RANGE.

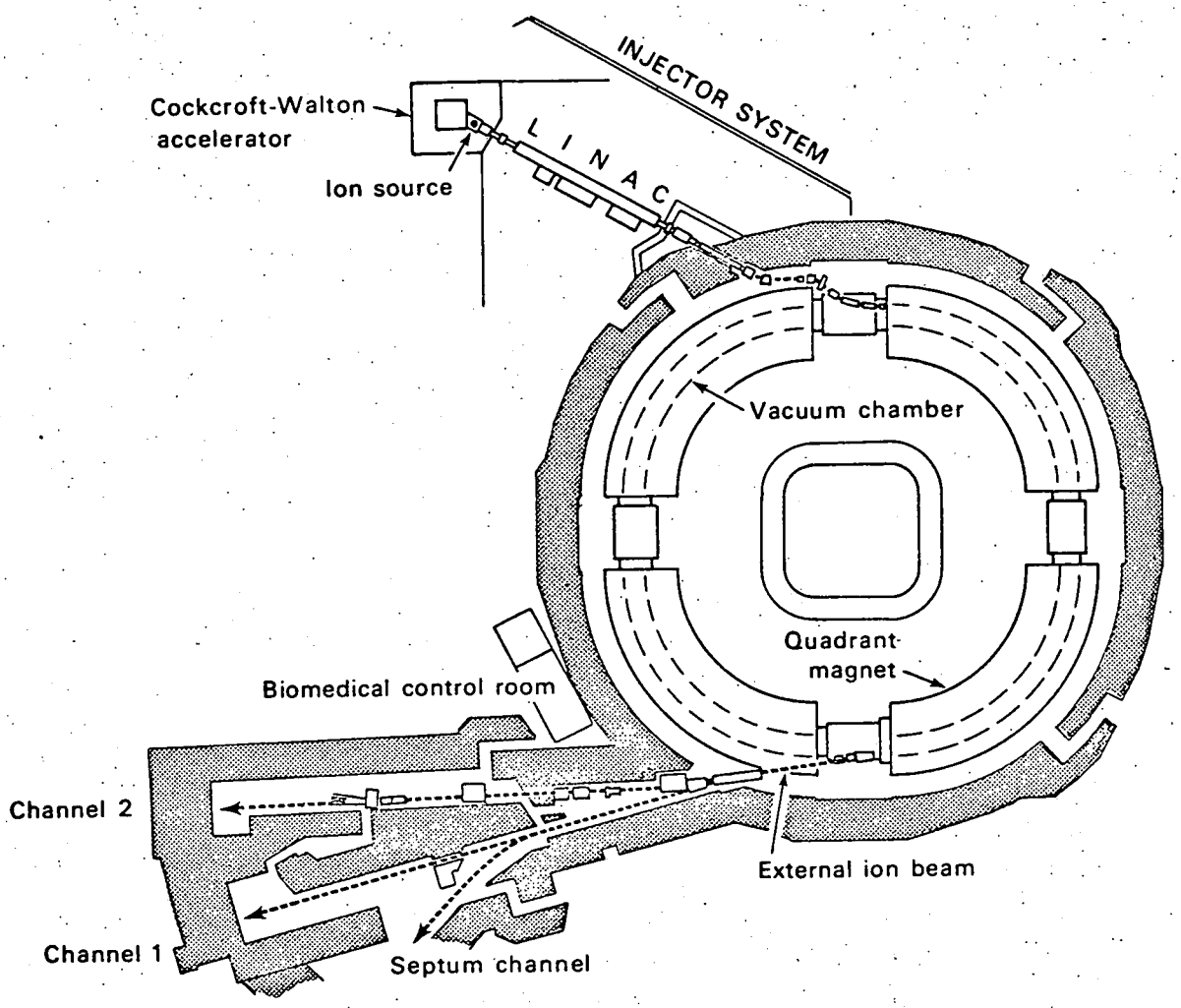

DBL 721 5108▲

Fig 1

SCHEMATIC DIAGRAM OF SILICON DETECTOR SYSTEM

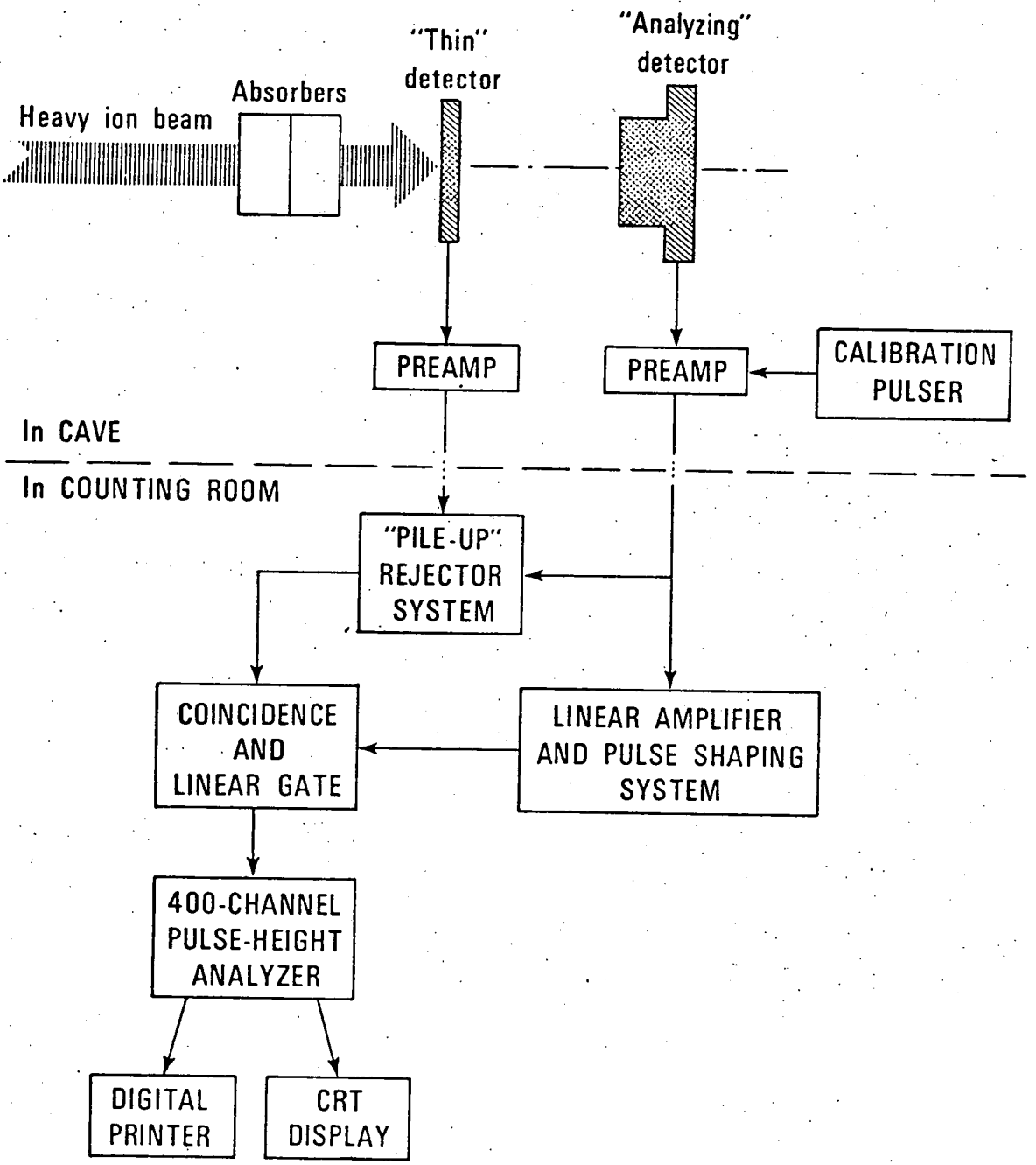

DBL 724 5243

Fig. 2

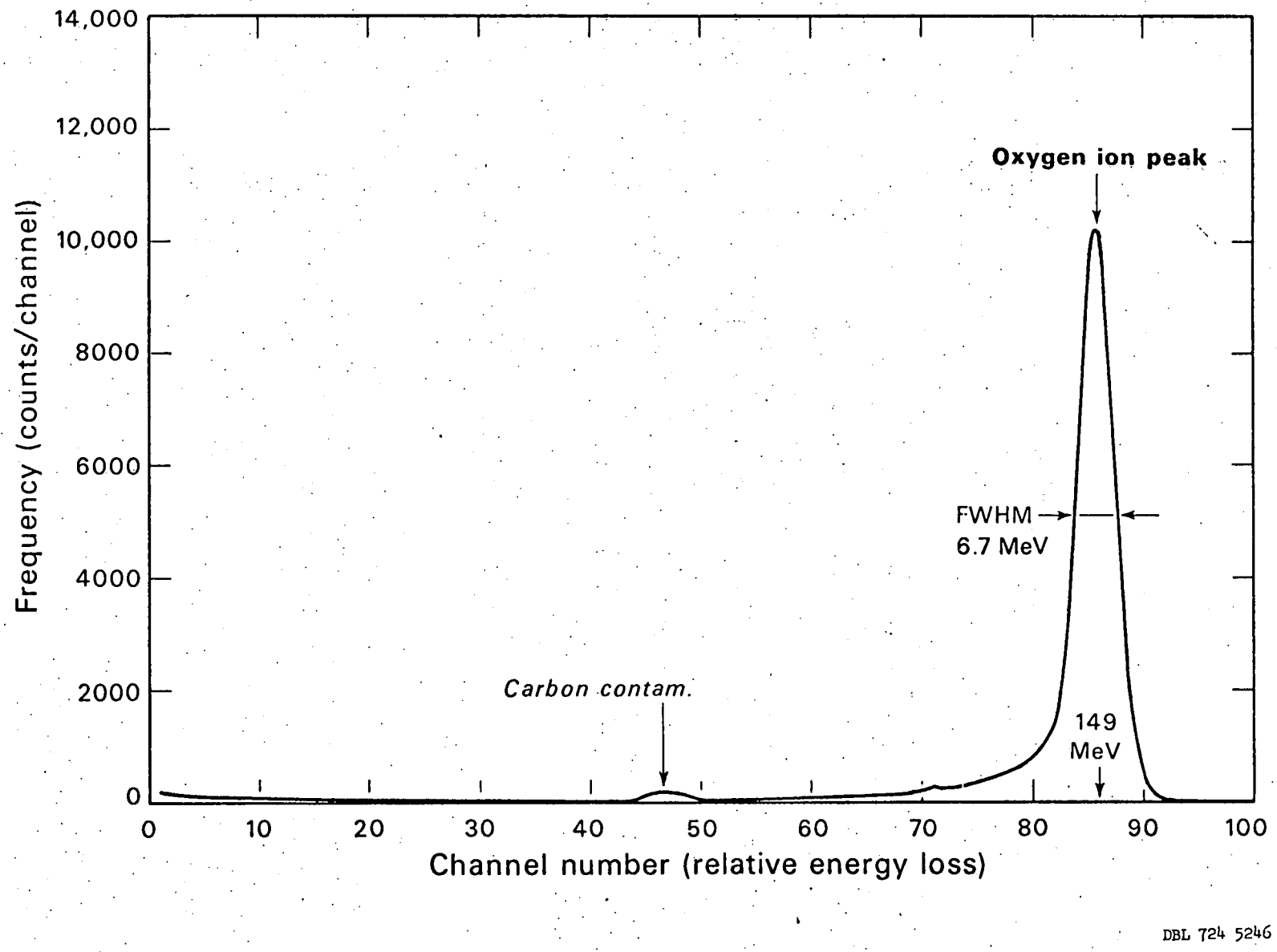
14,000
12,000
10,000
8000
6000
4000
2000
0
Frequency (counts/channel)
Oxygen ion peak
FWHM
6.7 MeV
Carbon contam.
149
MeV
0
10
20
30
40
50
60
70
80
90
100
Channel number (relative energy loss)
DBL 724 5246

Fig. 3

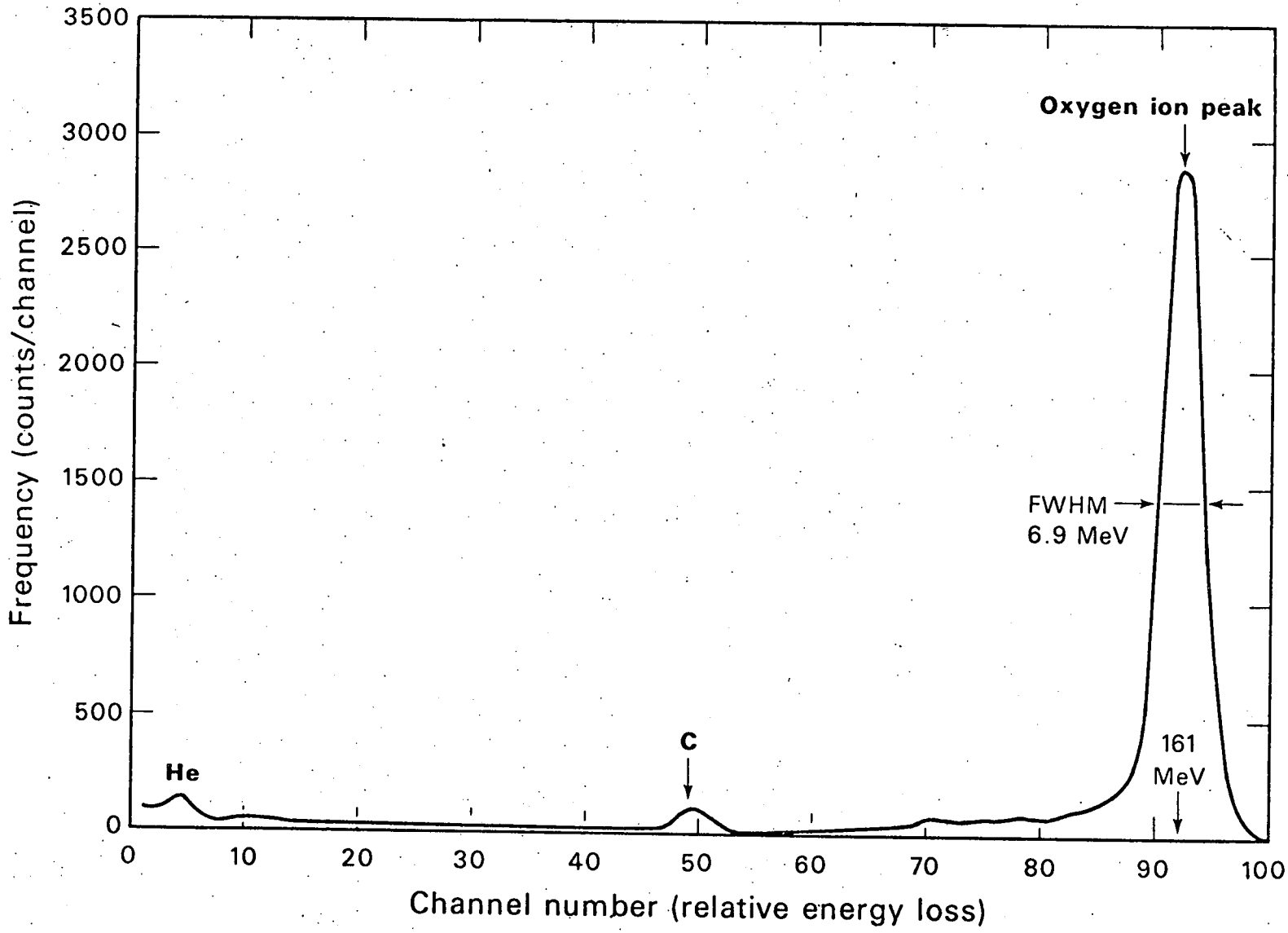

DBL 724 5245

Fig. 4

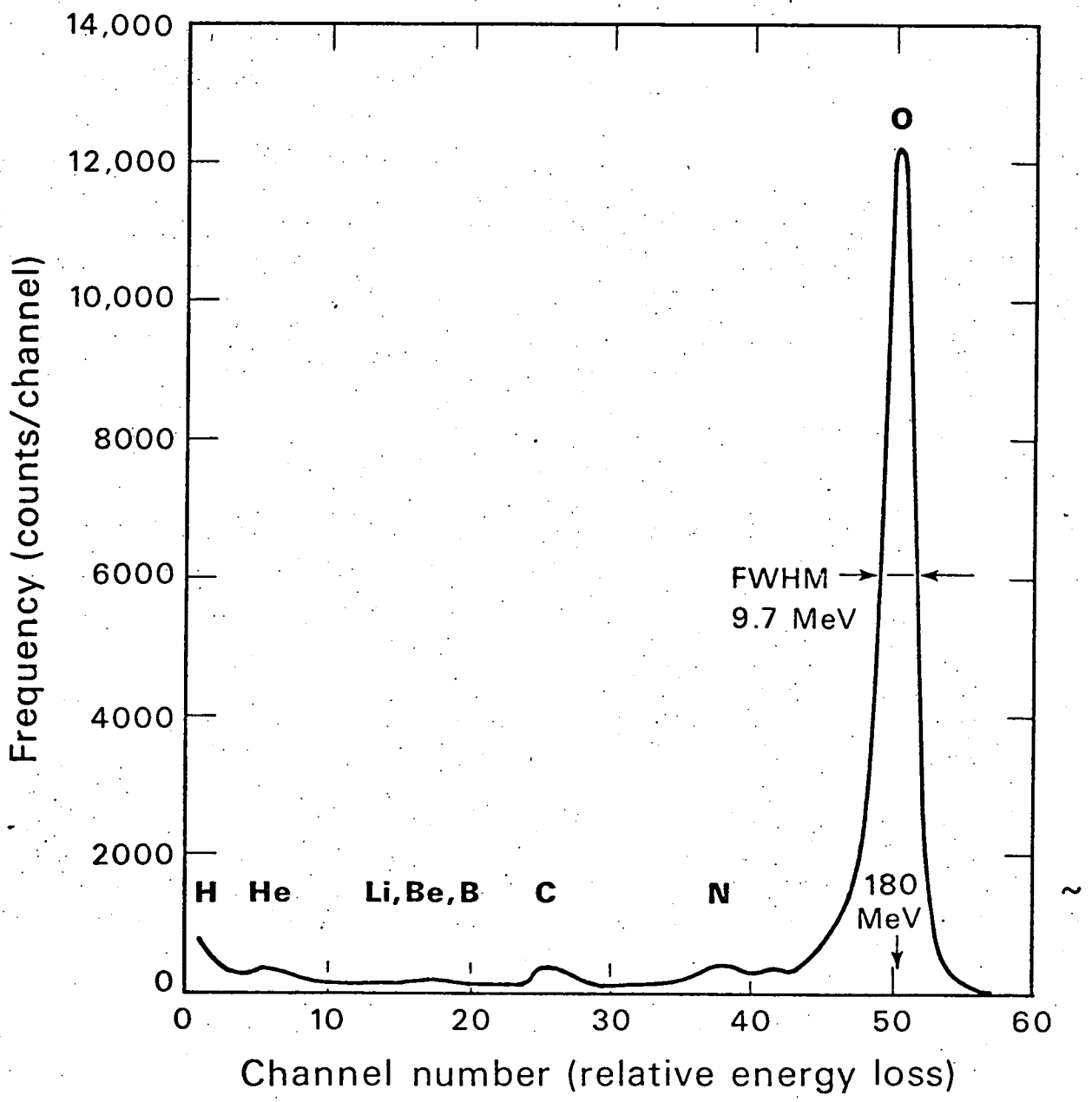

DBL 724 5244

Fig. 5

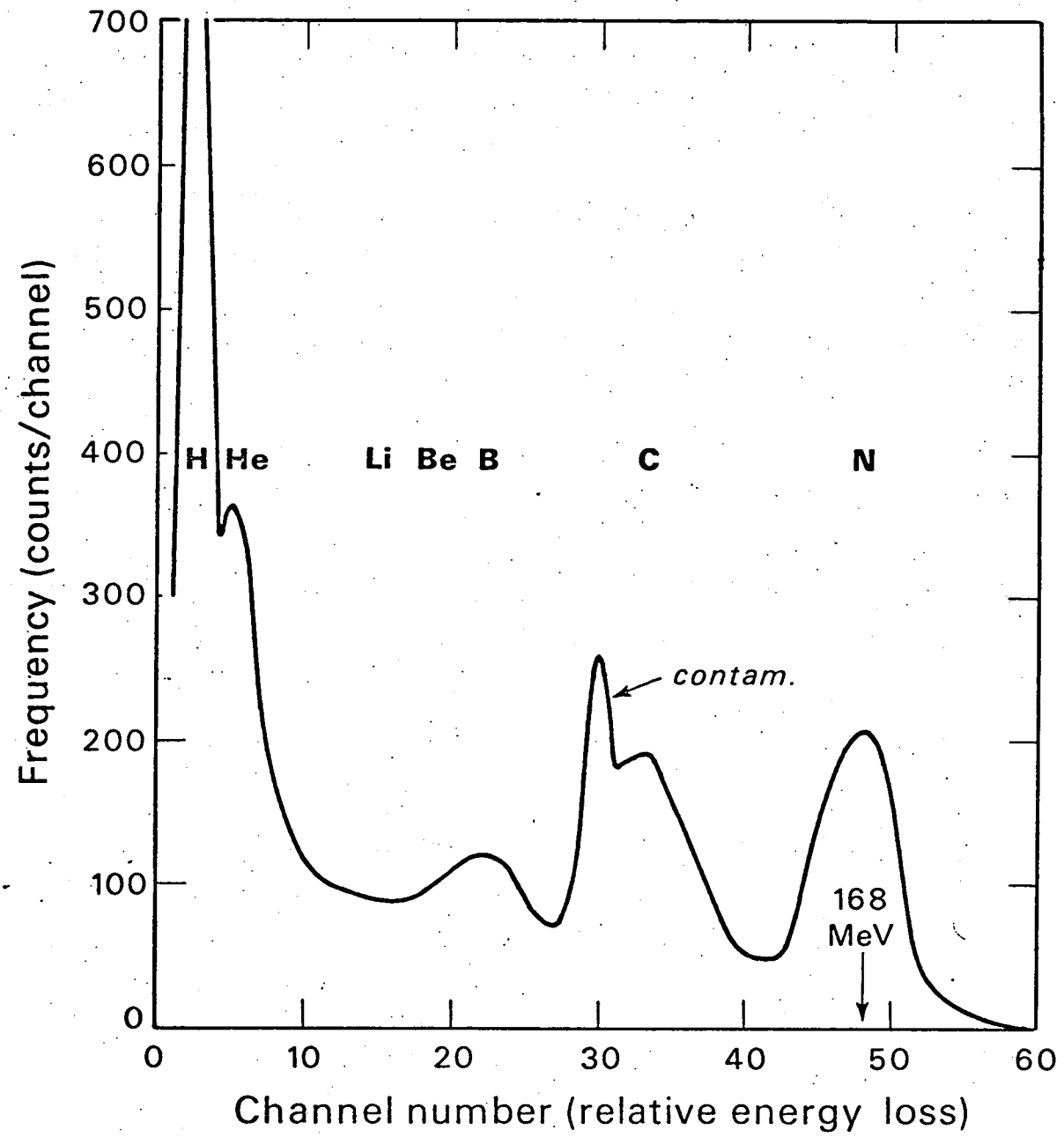

DBL 724 5247

Fig. 6

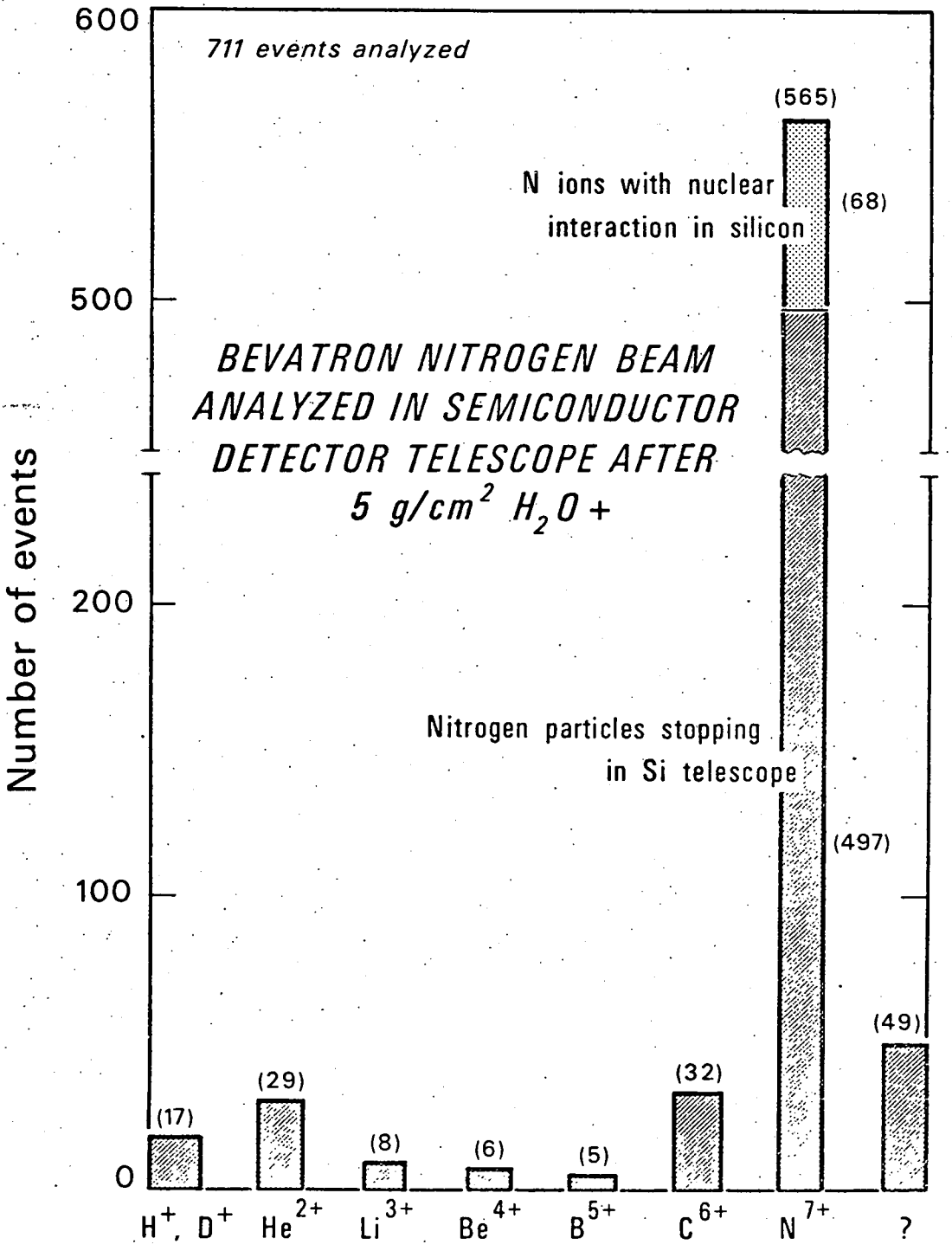
600
500
200
100
0
Number of events
711 events analyzed
(565)
N ions with nuclear interaction in silicon
(68)
BEVATRON NITROGEN BEAM ANALYZED IN SEMICONDUCTOR DETECTOR TELESCOPE AFTER 5 g/cm² H₂O +
Nitrogen particles stopping in Si telescope
(497)
(17)
(29)
(8)
(6)
(5)
(32)
(49)
H+, D+
He2+
Li3+
Be4+
B5+
C6+
N7+
?
DBL 7111 6091

Fig. 7

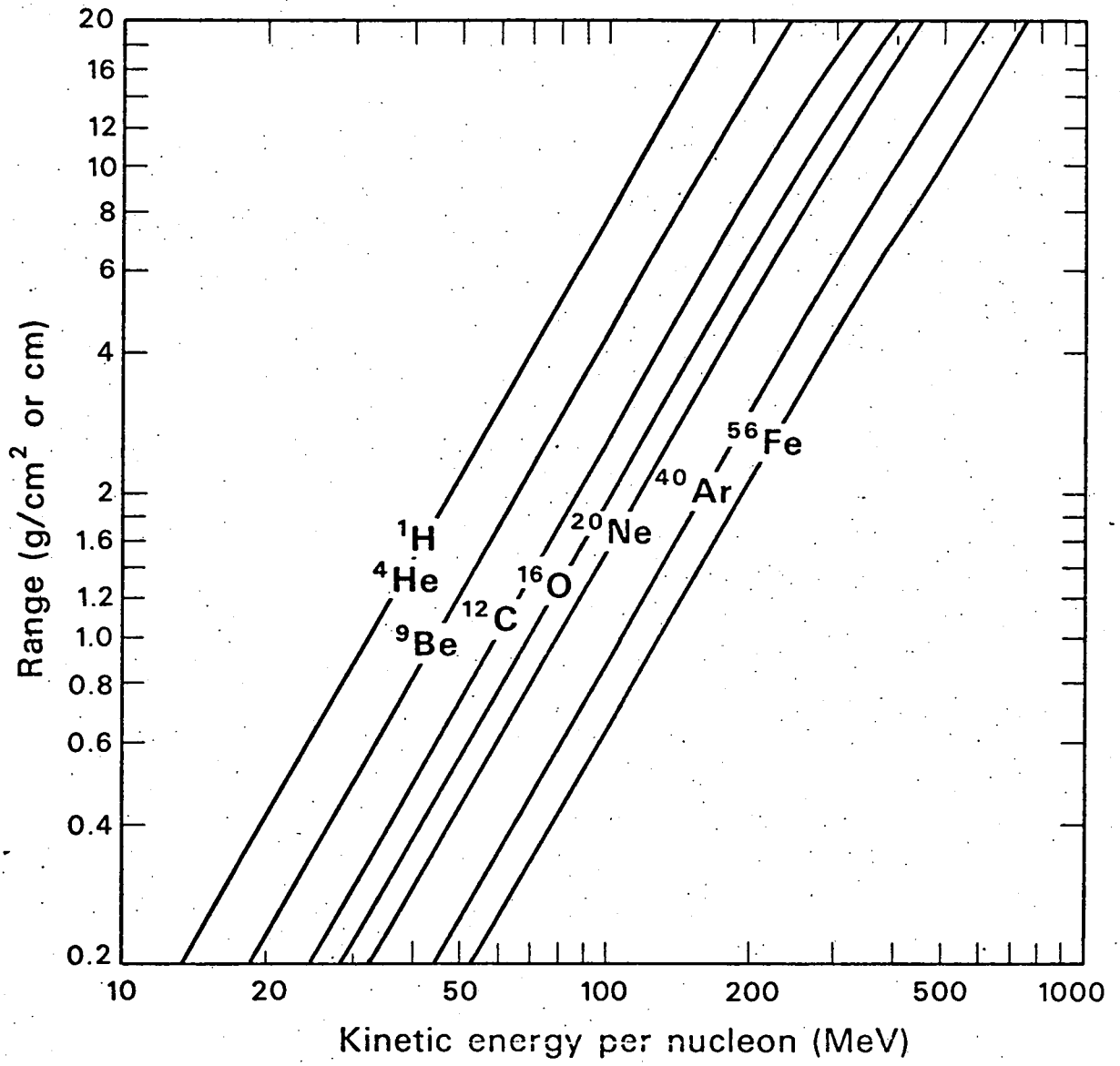

DBL 7212-5591

Fig. 8

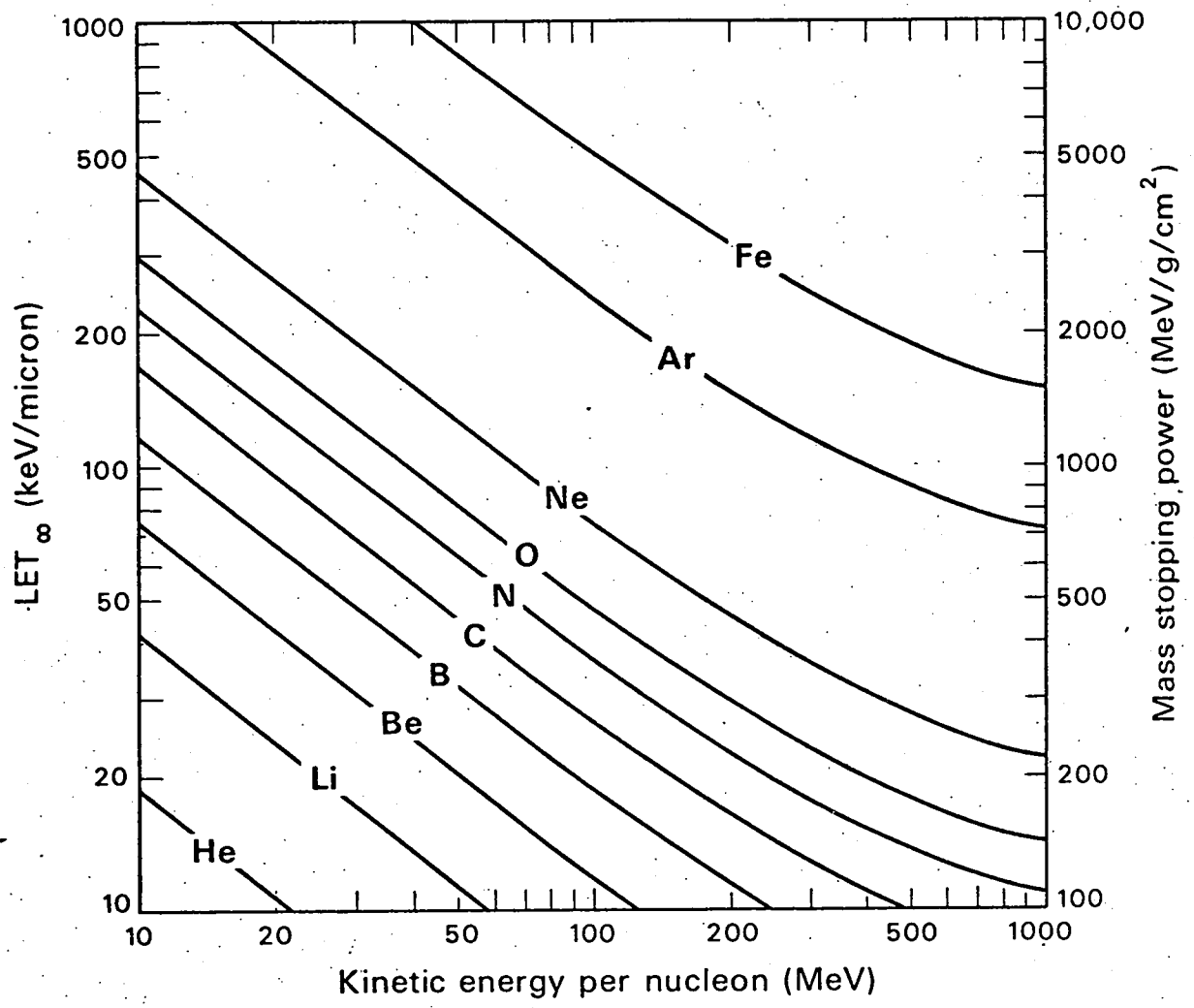

DBL 7212-5592

Fig. 9

Macalle

Information for Authors

Radiation Research

RADIATION RESEARCH will publish original articles in physics, chemistry, biology and medical research dealing with radiation effects and related subjects. The term *radiation* is used in its broad sense and includes specifically ultraviolet, infrared, and visible light as well as ionizing radiation. *Effects* may be physical, chemical, or biological. *Related subjects* include dosimetry, methods and instrumentation, isotope techniques, chemical agents, etc., contributing to the study of radiation effects. Book reviews are subject to restrictions as listed in *Radiat. Res.* **32,** p. 946, 1967.

Manuscripts offered for publication and books for review should be submitted to the Managing Editor, Oddvar F. Nygaard, Dept. of Radiology, Case Western Reserve University, Cleveland, Ohio 44106.

Manuscripts should not exceed 20 double-spaced typewritten pages with one-inch margins. The original and two copies complete with figures, tables, etc. should be included.

Each page of the manuscript should be numbered. The first page should contain the article, title and the author's name and complete address of laboratory of origin. At the bottom of this page, the number of copies submitted, manuscript pages, figures, and tables should be noted. The second page should contain a proposed running head of less than 35 characters. It should also contain the name and complete mailing address of the person to whom proofs are to be sent. The third page should contain an abstract of the paper. This abstract should not exceed 200 words and should be of the informative type. Complete sentences should be used and the use of proprietary terms and contractions should be avoided. A list of 3–5 key words for indexing should follow the abstract. The authors' names, title of the paper, and *Radiat. Res.*—, pp.—-—, —. should appear at the top of the abstract page. Further details appear in *Radiat. Res.* **28,** p. 726, 1966.

Tables are to be numbered consecutively in Roman numerals. Each table should be typed on a separate sheet, with due regard for the proportions of the printed page. Footnotes to tables should be identified by superscript letters and placed at the bottom of the page containing the table. Footnotes in the text should be identified by superscript numbers and listed consecutively on a separate page. Conclusions should be included at the end of the discussion.

All illustrations are to be considered as figures, and each graph, drawing, or photograph should be numbered in sequence with Arabic numerals. Each figure should have a legend, and these should be listed on a separate sheet. Figures should be planned to fit the proportions of the printed page (5 × 6¾ inches), and care should be taken that lettering on the original is large enough to be legible after reduction. Each figure should be identified in a margin with the name of the journal, the author's name, and the figure number. Graphs should be plotted on plain white or blue coordinate paper; grid lines that are to show in the engraving should be inked in black. Photographs should be submitted as glossy enlargements, and their number kept to the minimum. Illustrations should not exceed 8½ × 11 inches in size.

References should be cited in the text by number in parentheses (in order of appearance); author and year can be used in addition if of sufficient importance. The literature cited should appear on a separate page (*double spaced*) and should be listed consecutively according to reference number. Literature cited should be limited to material in the open literature; reports, private communications, etc. should be given as footnotes with adequate information as to their source and availability. Following the reference number, the author's initials, last name, title of reference, (capitalize first word only) journal name, volume, first and last page numbers, and year should be listed in that order. Abbreviations of journal names should follow the style of Chemical Abstracts' *Service Source Index* (1969 Edition). For book references, give the author's name, name of book, editor's name (if any), edition (if other than first), publisher's name, place, and year of publication.

Galley proofs will be sent to the author, together with reprint order forms and scale of reprint prices.

The author's institution will be asked to pay a part of the cost of publication in the form of a page charge of $10.00 per page which, if honored, entitles the institution to 100 free reprints. There will be no discrimination against papers for which the page charges are not paid.

Information for Authors

RADIATION RESEARCH will publish original articles in physics, chemistry, biology and medical research dealing with radiation effects and related subjects. The term *radiation* is used in its broad sense and includes specifically ultraviolet, infrared, and visible light as well as ionizing radiation. *Effects* may be physical, chemical, or biological. *Related subjects* include dosimetry, methods and instrumentation, isotope techniques, chemical agents, etc., contributing to the study of radiation effects. Book reviews are subject to restrictions as listed in *Radiat. Res.* **32,** p. 946, 1967.

Manuscripts offered for publication and books for review should be submitted to the Managing Editor, Oddvar F. Nygaard, Dept. of Radiology, Case Western Reserve University, Cleveland, Ohio 44106.

Manuscripts should not exceed 20 double-spaced typewritten pages with one-inch margins. The original and two copies complete with figures, tables, etc. should be included.

Each page of the manuscript should be numbered. The first page should contain the article, title and the author's name and complete address of laboratory of origin. At the bottom of this page, the number of copies submitted, manuscript pages, figures, and tables should be noted. The second page should contain a proposed running head of less than 35 characters. It should also contain the name and complete mailing address of the person to whom proofs are to be sent. The third page should contain an abstract of the paper. This abstract should not exceed 200 words and should be of the informative type. Complete sentences should be used and the use of proprietary terms and contractions should be avoided. A list of 3–5 key words for indexing should follow the abstract. The authors' names, title of the paper, and *Radiat. Res.*— , pp.— -— , — . should appear at the top of the abstract page. Further details appear in *Radiat. Res.* **28,** p. 726, 1966.

Tables are to be numbered consecutively in Roman numerals. Each table should be typed on a separate sheet, with due regard for the proportions of the printed page. Footnotes to tables should be identified by superscript letters and placed at the bottom of the page containing the table. Footnotes in the text should be identified by superscript numbers and listed consecutively on a separate page. Conclusions should be included at the end of the discussion.

All illustrations are to be considered as figures, and each graph, drawing, or photograph should be numbered in sequence with Arabic numerals. Each figure should have a legend, and these should be listed on a separate sheet. Figures should be planned to fit the proportions of the printed page (5 × 6¾ inches), and care should be taken that lettering on the original is large enough to be legible after reduction. Each figure should be identified in a margin with the name of the journal, the author's name, and the figure number. Graphs should be plotted on plain white or blue coordinate paper; grid lines that are to show in the engraving should be inked in black. Photographs should be submitted as glossy enlargements, and their number kept to the minimum. Illustrations should not exceed 8½ × 11 inches in size.

References should be cited in the text by number in parentheses (in order of appearance); author and year can be used in addition if of sufficient importance. The literature cited should appear on a separate page (*double spaced*) and should be listed consecutively according to reference number. Literature cited should be limited to material in the open literature; reports, private communications, etc. should be given as footnotes with adequate information as to their source and availability. Following the reference number, the author's initials, last name, title of reference, (capitalize first word only) journal name, volume, first and last page numbers, and year should be listed in that order. Abbreviations of journal names should follow the style of Chemical Abstracts' *Service Source Index* (1969 Edition). For book references, give the author's name, name of book, editor's name (if any), edition (if other than first), publisher's name, place, and year of publication.

Galley proofs will be sent to the author, together with reprint order forms and scale of reprint prices.

The author's institution will be asked to pay a part of the cost of publication in the form of a page charge of $10.00 per page which, if honored, entitles the institution to 100 free reprints. There will be no discrimination against papers for which the page charges are not paid.